Fast Charge Algorithm Development for Battery Packs under Electrochemical and Thermal Constraints with JModelica.org

Alberto Romero[1] Johannes Angerer[1]

[1]Kreisel Electric, Austria, {alberto.romero, johannes.angerer}@kreiselelectric.com

Abstract

Strict operating boundaries on commercial lithium ion cells are defined to mitigate the effect of aging and avoid safety hazards like, the appearance of lithium plating during fast charge, which can lead to internal short circuit and subsequent thermal runaway. Most studies so far have focused on the single cell charging problem because the temperature difference between cells within a battery pack is often considered small, and therefore optimal charging profiles can be extrapolated from single cell investigations. In practice, temperature spread can reach up to 10 K from coldest to warmest points in the pack, and at least 5 K between same position of different cells. With this in mind, a Nonlinear Model Predictive Control (NMPC) scheme is proposed that considers both electrochemical and thermal constraints at pack level, establishing, at least on a theoretical basis, the practical limits of fast charge. An electrochemical cell model and the pack thermohydraulic balance equations were modeled using Modelica. The NMPC implementation is carried out using JModelica.org to find the optimal control actions, and includes the closed loop control problem on a high fidelity plant model. We demonstrate how active thermal management, i.e., controlling the fluid inlet temperature, is critical to reducing charging times below 40 min (from 5% to 80% state of charge), and discuss some challenges when using online optimization-based control techniques.

Keywords: Li-ion battery pack, fast charge, constrained control, temperature spread, FMI

1 Introduction

The performance and lifetime of lithium-ion battery packs strongly depend on the operating conditions, typically determined and/or limited by the user's needs and the auxiliary systems, i.e., the thermal management system (TMS) and the battery management system (BMS). Moreover, operating limits and control strategies may change over time to accommodate for changes in the battery state of health (SOH). Therefore, an operating strategy that meets the required performance and lifetime must be established around the individual cells, the packs built upon them, and the subsystems responsible for adjusting the boundary conditions and applying the constraints under which cells operate.

1.1 Compromises between performance and lifetime

The battery operation strategy modifies or adjusts the performance in the short term, for example, tightening the operating power envelope, thus reducing peak temperatures, in order to achieve a desired lifetime (Barreras, Raj, and Howey 2018). Another example of adjusting thermal and electrochemical limits is the so-called extreme fast charge (XFC) (Yang, T. Liu, et al. 2019), where the cell operating temperature is increased to enhance the electrochemical dynamics to ensure safety requirements. The negative effect in lifetime of higher temperatures is compensated by a significant shorter charging times, which is considered a critical requirement in certain applications, like electric vehicles (EV).

1.2 Temperature limits for commercial Li-ion cells

Modern lithium-ion cells can nevertheless operate over a wide range of temperatures, typically from -30°C to 60°C. A common upper limit of commercial cells can be found around 80°C (Groß and Golubkov 2021), while the Department of Energy of the United States (DOE) established the maximum operating cell temperature at 52°C (Keyser et al. 2017). But already within these limits, and especially beyond them, different degradation mechanisms lead to the progressive deterioration of the performance, reducing the life time of the cells beyond practical or economical criteria. According to information summarized in (Keyser et al. 2017), cell lifetime doubles approximately for each 13K temperature reduction: if 10 years of lifetime is achieved operating at 20°C, the same cell under the same current load would last less than 5 years at 35°C.

Early studies on lithium-ion batteries established the ideal operating temperature range between 25°C and 40°C for a *"good balance between performance and life*", as well as a module to module temperature spread below 5K (A. A. Pesaran 2002). More recently, temperature limitations have been established using different guidelines to improve safety and performance: maximum temperature 40°C, minimum temperature -30°C, maximum (internal cell) temperature difference 10K, and mean temperature between 25°C and 30°C (M. Sievers, U. Sievers, and Mao 2010).

Recent efforts in quantifying the actual thermal performance of battery packs have been done. Wassiliadis et al.

(2022) determined that sensors located at different cells within a battery module of an electric vehicle (with bottom plate liquid cooling) measured a temperature spread below 2 K during a DC fast charging (maximum C-rate below 1C). Given the large cell format of their test, the maximum difference between the coldest and warmest points of the module (i.e., the absolute difference) could indeed be closer to the difference between cell sensors and fluid inlet temperature, which for their fast charge test is a difference of up to 20 K. On a similar but only simulated case, J. Wang et al. (2020) report between 3.5 and 5 K absolute difference during a 2C discharge depending on the design of the cooling channels and the mass flow rate of the fluid. In practice, absolute temperature spread in real packs are likely to reach 10 K, although efforts to keep it below 5 K is the general consensus, whether absolute or cell to cell spread.

1.3 Solving the fast charge problem

Temperature limits during charge may differ significantly from those while discharging due to the possibility of lithium plating. This negative side-reaction usually takes place at low temperatures, but it can also appear at room temperature for moderate to high charging C-rates (Yang and C.-Y. Wang 2018). As indicated by Yang, T. Liu, et al. (2019), it is desirable to relax the upper temperature limits while charging in order to improve performance at the expense of a marginally higher aging to ensure safety.

The problem fast charge (i.e., how to tackle its complexity and produce safe and fast charge profiles) has been addressed in the literature with different methods, and today vehicle manufacturers have developed practical approaches that consider not only the battery limits, but also the TMS, BMS, on-board converters, power grid (and charger), the local environmental conditions and the user driving needs. The scientific literature has mainly addressed the fast charge problem at cell level (for an application in Modelica, see Romero, Goldar, and Garone (2019)), but studies at pack level that address the effect and limits of TMS are less abundant.

With exclusive focus on cell level fast charge, recent efforts on cell modelling in various spatial and physic domains have led to the conclusion that Li-ion cells can be safely charged below 20 min (0-80% SOC). Frank et al. (2022) established (simulation results only) a theoretical minimum of 18 min for 18650 and 21700 cylindrical cells with conventional tab design, and 13 min for the larger 4680 format with tabless technology; according to the authors, cooling limitations bring the values closer to 20 min and 16 min, respectively. However, the anode potential constraints are set to 0 mV, which leaves no safety margin for the possibility of lithium plating. With the purpose of avoiding lithium plating through a safety buffer (e.g., 20 mV) Yin and Choe (2020) optimized a combined fast charge profile with periodical discharge pulses that favour lithium stripping, i.e., the recovery of already plated lithium. Together with offline and online optimization methods, which include the selection of the optimal temperature boundary, the authors prove experimentally that 18 min is possible (0-80%) with lifetime degradation similar to 1C CCCV (1C constant current, followed by constant voltage) protocol (47 min, 0-80%). It is in general acknowledged, nevertheless, that these fast charge speeds are hardly attainable at pack level, where cell heterogeneities and challenges cooling technologies play a critical role (Tomaszewska et al. 2019).

Modelica has seen a growing number of libraries and studies dedicated to battery systems. The reader is referred to validated libraries reported in Dao and Schmitke (2015), Uddin and Picarelli (2014), Gerl et al. (2014), Bouvy et al. (2012), Brembeck and Wielgos (2011), Einhorn et al. (2011), and Janczyk et al. (2016), as well particular applications on fuel economy (Batteh and Tiller 2009; Spike et al. 2015), thermal management (Bouvy et al. 2012), cell modelling and coolant analysis (Krüger, M. Sievers, and Schmitz 2009),and battery aging (Gerl et al. 2014; Stüber 2017). More recently, (Groß and Golubkov 2021) developed a comprehensive Li-ion library that includes not only electrical cell models, but also thermal runaway (TR) and propagation dynamics, i.e., equations that capture the chemical reactions once an onset temperature is reached.

Completing the single cell level optimal charging analysis presented in (Romero, Goldar, and Garone 2019), this work addresses the limits of fast charge at pack level on an immersion cooled battery with dielectric fluid under electrochemical and thermal constraints. Such cooling approach puts the fluid in direct contact with the cells, which results in higher heat transfer compared to indirect cooling. We make use of Model Predictive Control (MPC) (Camacho and Alba 2013), implemented using the tool JModelica.org (Andersson et al. 2011; Magnusson and Åkesson 2015). A validated functional mock-up unit (FMU) (Blochwitz et al. 2011) is used as a plant model, while a simplified, yet nonlinear model of the pack written in the Modelica language with the same inputs (current, fluid flowrate and inlet temperature) is considered.

The reminder of the paper is organized as follows. Section 2 describes the electrochemical cell model used to model the internal states associated to lithium plating. Section 3 introduces the proposed MPC scheme, describing the cost function, the prediction model, and the plant model. The first part of section 4 explores the optimal profiles under a different set of constraints solved as an offline optimization problem, and then presents the NMPC results accompanied with a discussion related to constraints saturation. This paper is closed with the conclusion section completed with future paths to be investigated.

2 Electrochemical cell model

To support its development activities around battery pack design and simulation, Kreisel Electric (2023) has been working with different Li-ion cell model paradigms, in-

DOI 10.3384/ecp204121

cluding Equivalent Circuit Models (ECM), Equivalent Hydraulic Model (EHM), Single Particle Model (SPM), and higher level detail models like the P2D Neuman-Fuller-Doyle model. For most of the electrothermal simulations, we rely on ECM-based battery packs, and resort to the light weight EHM when some electrochemical state information is needed, for example in fast charge analyses, the focus of the present paper.

The EHM is based on the original work of (Manwell and McGowan 1993), where the hydraulic analogy is used to describe the dynamics of charge moving between volumes of active material. One recent use of this analogy on Li-ion batteries was proposed by Couto et al. (2016), although derivations of similar models can be found in different sources (Y. Li et al. 2019). The EHM is equivalent to the second order Padé approximation and valid for current pulses with frequencies below 0.5mHz (0.002rad/s) (Forman et al. 2011). Knowing that the 1C/1C cycle results in a frequency of 0.14mHz (charge and discharge included, 1h long each), aging protocols including high charging, steady currents of up to 3.6C fall well under the validity range of the EHM to accurately predict lithium plating.

Consequently with the model choice, the following assumptions must be considered:

1. 0D electrochemical and thermal dynamics
2. Homogeneous behaviour in electrode and separator
3. Fast positive electrode dynamics
4. Constant lithium concentration in electrolyte
5. Temperature dependent exchange current density
6. Heat transfer dominated by side liquid cooling

The EHM considers two electrochemical states, the bulk concentration and the surface concentration, in representative solid particles of the positive and negative electrodes. They are normalized with the maximum concentration ($c_{s,max}$) and denoted by SOC and CSC respectively. The model considers as input the normalized current (I) using the electrode area (A_{cell}), to provide a form factor independent calculation.

$$\frac{d\,\mathrm{SOC_n}}{dt} = -\gamma I \tag{1}$$

$$\frac{d\,\mathrm{CSC_n}}{dt} = \frac{g}{\beta(1-\beta)}\left(\mathrm{SOC_n} - \mathrm{CSC_n}\right) - \frac{\gamma}{1-\beta} I \tag{2}$$

$$\mathrm{SOC_p} = \rho\,\mathrm{SOC_n} + \sigma \tag{3}$$

$$\mathrm{CSC_p} = \mathrm{SOC_p} \tag{4}$$

$$V = U_\mathrm{p} - U_\mathrm{n} + \eta_\mathrm{p} - \eta_\mathrm{n} - (R_\mathrm{f} + R_\mathrm{cc} A_\mathrm{cell})\, I \tag{5}$$

$$V_\mathrm{n} = U_\mathrm{n} + \eta_\mathrm{n} \tag{6}$$

$$\eta_\mathrm{p,n} = \frac{RT}{\alpha F} \sinh^{-1}\left(\frac{\theta_\mathrm{p,n} I}{\sqrt{\mathrm{CSC_{p,n}}\left(1-\mathrm{CSC_{p,n}}\right)}}\right). \tag{7}$$

Table 1 summarizes the most relevant model parameters and exact or reference values for energy cells (C.-H. Chen et al. 2020). The actual values of such parameters used in this work are not disclosed. Moreover, since the diffusion dynamic of the cathode is assumed to be orders of magnitude faster, only the negative electrode is modelled.

Table 1. Cell model parameters

Parameter	*Units*	Value
Particle radius, R_s	$[\mu m]$	5
Electrode thickness, l	$[\mu m]$	80
Diffusion coefficient, D	$[m^2/s]$	1e-15
Active material vol. fraction, ε	%	75
Specific interfacial area, a	$[m^2/m^3]$	45e3
Effective reaction rate, r_{eff}	$[\frac{A}{m^2}(\frac{m^3}{mol})^{1.5}]$	7e-6
Maximum concentration $c_{s,max}$	$[mol/m^3]$	30e3
Electrolyte concentration, c_{e0}	$[mol/m^3]$	1200

The relationships of these parameters with the proper parameters of the EHM system are the following

$$\gamma = \frac{3}{R_\mathrm{s}\, a F\, l\, c_\mathrm{s,max}} \quad g = \frac{147}{20}\tau \quad \beta = \frac{7}{10}$$

$$\tau = \frac{R_\mathrm{s}^2}{D} \qquad a = 3\frac{\varepsilon}{R_\mathrm{s}} \qquad \theta = \frac{1}{2\, a\, l\, r_\mathrm{eff}\, c_\mathrm{e0}^{1/2}\, c_\mathrm{s,max}}.$$

For more information regarding the cell electrochemical models and the equations used in this paper the reader is referred to Romero, Goldar, and Garone (2019), Dao and Schmitke (2015), Chaturvedi et al. (2010), and M. Sievers, U. Sievers, and Mao (2010).

The thermal model assumes lumped properties collapsing on the cell centre, i.e., the warmest area. The thermal resistance consists of a serial sum of convection and conduction terms (external and internal heat flow respectively)

$$m_\mathrm{cell} C_\mathrm{p,cell} \frac{dT}{dt} = i\,(V - (U_\mathrm{p} - U_\mathrm{n}) + T\,(\frac{\partial U_\mathrm{p}}{\partial T} - \frac{\partial U_\mathrm{n}}{\partial T})) \quad -\frac{1}{R_\mathrm{th}}(T - T_\mathrm{amb}) \tag{8}$$

$$A = \pi D H_\mathrm{c} \quad R_\mathrm{th} = (\frac{1}{4\pi H_\mathrm{c} k} + \frac{\ln(D_\mathrm{can}/D))}{2\pi H_\mathrm{c} k_\mathrm{can}} + \frac{1}{hA}) \tag{9}$$

where R_th is the thermal resistance of the lumped thermal model of the cell, h is the heat transfer coefficient w.r.t. the liquid cooled section, and $\frac{\partial U_\mathrm{p(n)}}{\partial T}$ define the so called entropic heat of the positive (negative) electrode (Dao and Schmitke 2015). We note here that this model approximates the behaviour of an infinite cylinder with homogeneous heat generation. In reality, the active cooled

length is limited to a portion of the total height of the cell, while the rest is cooled passively by natural convection with the surrounding air. The can conductivity is high enough, and its thickness is so small, as to neglect its contribution in the total resistance. The entropic heat, as well as the heat transfer to the air, are also considered negligible. Thus, the simplified model can be reduced to

$$m_{\text{cell}} C_{\text{p,cell}} \frac{dT}{dt} = i(V - (U_{\text{p}} - U_{\text{n}})) - UA(T - T_{\text{amb}}), \tag{10}$$

where U is the so called overall heat transfer coefficient.

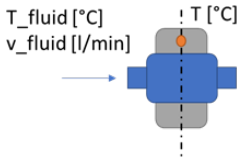

Figure 1. Single Cell thermal model.

3 Model Predictive Control scheme

MPC has been selected as a control paradigm to adjust the inputs, denoted as $u(t)$, which in the general case of a battery pack operation with liquid cooling consists of current, fluid flowrate and fluid inlet temperature. Additional, non-manipulated inputs or disturbances, can be the ambient temperature or the parasitic loads connected to the battery pack. For simplicity, we neglect the effect of the latter, and limit the control inputs to the battery current and the fluid inlet temperature. Moreover, we consider that internal states are observable in practice, but in a real implementation a well tuned estimation method (e.g., Kalman-Filter) must be used.

The nature of the system is non-linear, not only from the coupling between electrochemical and thermal model (the heat source is proportional to i^2, i being the current of the cell or pack), but also because the product of flowrate (considered however constant in the present work) and temperature difference in the heat exchanged. The latter can be simplified for the single cell case, and decoupling and linearisation of the state space system could be solved in a decentralized fashion as reported in Romero, Goldar, Couto, et al. (2019). Therefore, in general, non-linear solvers are needed in the optimization problem, specially when pack-level control is considered.

3.1 Optimization problem

The on-line nonlinear optimization problem subject to constraints that can be written as

$$\begin{aligned} \min_{u(t)} \quad & \int_{t_0}^{t_{\text{f}}} [(\text{SOC}(t) - \text{SOC}_{\text{ref}})^2 + k_{\text{T}}(\text{T}(t) - \text{T}_{\text{init}})^2] dt \\ \text{s.t.} \quad & \text{model dynamicsconstraints} \\ & \text{electrochemical constraints} \\ & \text{thermal constraints.} \end{aligned} \tag{11}$$

The first row in Equation 11 is the integral cost over the horizon determined between t_0 and t_{f}. Its first term penalizes the difference between the SOC at time t and the desired reference SOC_{ref}. An additional cost term is added to bring the cell/pack temperature to a desired value for storage or before discharge begins. In addition to the model dynamics itself, two type of constraints are considered: electrochemical constraints on the anode potential (V_{n}) to avoid lithium plating, and thermal constraints including maximum and minimum cell temperature (T_{max}, T_{min}), as well as maximum temperature spread within the pack (T_{spread}).

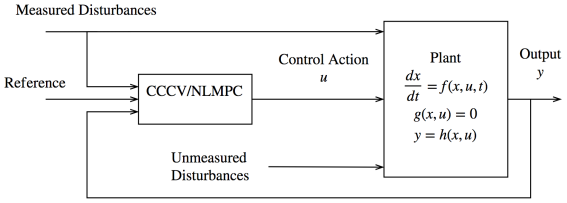

Figure 2. Model Predictive Control Scheme

3.2 Prediction Model

The optimization class extends the pack model `PackEHMT`, i.e., the prediction model, which includes all state and output dependencies with the input variables. The following listing is part of the optimization class `EHMTVpack_OptMPC`, which includes a constraint section that defines the limits of operation for the cell and pack.

Listing 1. Optimization class `EHMTVpack_OptMPC`

```
optimization EHMTVpack_OptMPC (
   objectiveIntegrand =
     (SOC - SOC_ref)^2 + 1e-8*(T-T_init)^2,
   startTime = 0, finalTime = 1000)

  extends PackEHMT(
    CSC(fixed=true), CSCn_0=0.05,
    SOC(fixed=true), SOCn_0=0.05,
    T(fixed=true), Tm(fixed=true),
    Tf(fixed=true), T_init = 298.15);
  // ...

  // Example of limit values:
  parameter Real SOC_ref = 0.80;
  parameter Real SOC_max = 0.65;
  parameter Voltage V_max = 4.2;
  parameter Temperature T_max = 450;
  parameter Temperature Tf_max = 450;
```


DOI 10.3384/ecp204121

```
  parameter Temperature Tspread_max = 10;
  parameter Temperature DTf_low = 10;
  parameter Temperature DTf_high = 25;
  parameter Current i_max = 20;
  parameter Voltage Van_min = 0.1;

equation
  U_n = ...;
  U_p = ...;
  Van = R * T / alpha / F * Modelica.Math.
      log(theta_n * (I) / sqrt(CSC * (1 -
      CSC)) + sqrt(1 + (theta_n * I / sqrt(
      CSC * (1 - CSC))) ^ 2)) + U_n;

constraint
  SOC <= SOC_max;
  CSC <= SOC_max;
  SOC >= 0.0001;
  CSC >= 0.0001;
  Van >= Van_min;
  Tfin >= T_amb - DTf_low;
  Tfin <= T_amb + DTf_high;
  (Tf - T) <= Tspread_max;
  -(Tf - T) <= Tspread_max;
  i <= i_max;
  T <= T_max;
  Tf <= Tf_max;
  V <= V_max;

end   EHMTVpack_OptMPC;
```

The core model of the battery pack is the cell model `CellEHMT_base`, where the main electrical and electrochemical parameters and equations are defined. The only exception is lack of a cell temperature model. This and the temperature balances of the full pack form the model class `PackEHMT` as shown in Listing 2. Figure 3 shows the approach to simplify the pack equations, where the cells between the first and last are lumped into a single thermal node. Despite its simplicity, this approximation allows us to obtain an inlet fluid temperature for the last cell, and yields a level of fidelity for the pack model sufficiently accurate for an MPC scheme.

Listing 2. Pack model class `PackEHMT`

```
model PackEHMT

  extends CellEHMT_base; // includes state
      variable T
  //...
  parameter Integer nmid = 400 "Cells in
      the middle";
  Power Q(start = 0);
  Power Qm(start = 0);
  Power Qf(start = 0);
  Temperature Tf2(start = T_init);
  Temperature Tf3(start = T_init);
  Temperature Tf4(start = T_init);
  Temperature Tm(start = Tm0) "Temperature
      cells in the middle";
  Temperature Tf(start = Tf0) "Temperature
      last module cell";
  parameter MassFlowRate mfr = 0.001 "Mass
      flow rate";
  inputTemperature Tfin "Inlet fluid
      temperature";

equation
  //...
  V = U_p - U_n + ...;
  Q = 1/(1/(h * A) + 1/G_rad)*(T-(Tfin+Tf2)
      /2);
  Q = mfr*Cpf*(Tf2-Tfin);
  Qm = nmid*1/(1/(h * A) + 1/G_rad)*(Tm-(
      Tf3+Tf2)/2);
  Qm = mfr*Cpf*(Tf3-Tf2);
  Qf = 1/(1/(h * A) + 1/G_rad)*(Tf-(Tf4+Tf3
      )/2);
  Qf = mfr*Cpf*(Tf4-Tf3);
  P_loss =  i * (V - U_p + U_n);
  der(T) = (P_loss - Q)/(M*Cp);
  der(Tm) = (nmid*P_loss - Qm)/(M*Cp*nmid);
  der(Tf) = (P_loss - Qf)/(M*Cp);

end PackEHMT;
```

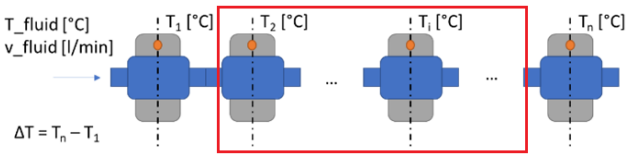

Figure 3. Simplified pack model with lumped dynamics within the rectangle.

3.3 Plant Model

For the plant model, a high definition, 1D battery pack nonlinear model is used. The pack consists of several stacks connected hydraulically in parallel and electrically in series. Each stack consist of several modules, made of staggered groupings of 36 cells secured within a cooling enclosure, which allows for a dielectric fluid to circulate in contact with the surface of the cells using immersion cooling technology (Kastler and Menzl 2021). More information about a similar stack can be found in the work of Kasper et al. (2023).

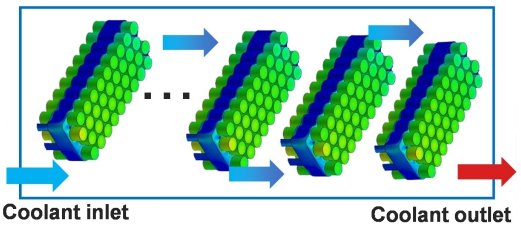

Figure 4. Stack formed by a variable number of modules

The maximum voltage of the pack's energy content is 60 kWh. A detailed view of an arbitrarily long stack is shown in Figure 4. This pack model, of which an FMU was created and integrated in the main simulation loop, uses a validated ECM cell model without aging dynamics, with a discretized model consisting in 9 sub-volumes (3 divisions in radial direction and 3 in axial).

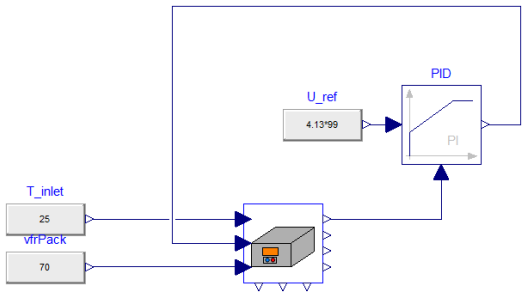

Figure 5. Pack model tested with a CCCV charge using a limited PI

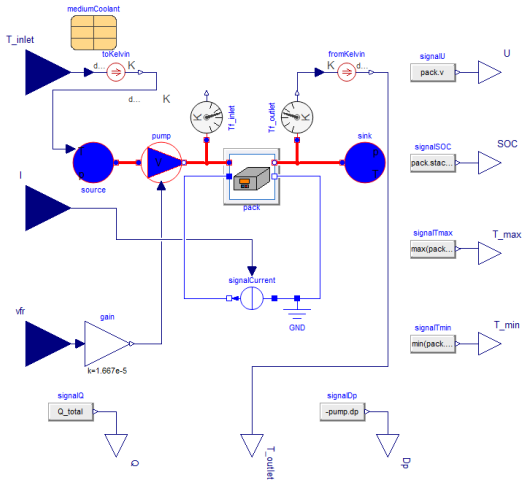

Figure 6. Pack model interface detail

4 Case studies

To illustrate what an optimal operation strategy looks like and how it is calculated, a series of optimization problems are solved, first solving the off-line, fast charge problem, and then a closed-loop NMPC with state feedback on a realistic plant model. We are concerned in this work with the optimal charge, i.e., the overall control strategy including the discharge phase of the cycle is part of ongoing investigations. The main control parameters needed in JModelica.org are shown in Table 2.

First, the optimal constrained fast charge profile of a 5 Ah, 21700 format cylindrical single cell with immersion cooling is computed and compared with standard charging protocols with passively cooled cell. The optimization is carried out under several constraints involving voltage, temperature, and electrochemical limits, that prevent premature aging and lithium plating. Subsequently, the optimal profile for the battery pack, based on the same cell, is calculated without and with additional temperature spread limit. In all cases the same `EHMTVpack_OptMPC` class, where only the constraints (upper and lower values) are adjusted for each of the cases described.

Table 2. NMPC controller setup

Variable	*Value*	*Units*
t_f	1000	[s]
SOC_{ref}	0.665	[-]
n_e	100	[-]
n_{cp}	1	[-]
H	1000	[s]
Δt_{MPC}	10	[s]
Δt_{sim}	1	[s]
solver	IPOPT	

Finally, the NMPC scheme proposed in the previous section is used to determine the impact of imperfect state feedback and control horizon on the constraint satisfaction and the controller performance.

4.1 Single cell optimal charge

We begin by comparing the conventional charge protocol in three basic situations: passive cooling with 1C charge CCCV, and immersion cooling at different C-rates: 1C/2C CCCV. Passive cooling is defined by a boundary condition defined by the overall heat transfer coefficient (U) equal to 1 W/m^2K over the whole surface of the cell, which is the case of a slightly insulated cell subject to natural convection heat transfer. For immersion cooling, a value of U = 200 W/m^2K has been chosen.

4.1.1 Cooling system comparison

Figure 7 illustrates a typical 1C-CCCV charge profile of a commercial Li-ion cell. Starting at 7.5% SOC, it reaches 80% in 45 min. From top to bottom, the subplots contain state of charge and critical surface concentration (expressed as percentage at target SOC stoichiometric), current and voltage, anode potential, and cell temperature. Passively cooled cells experience high peak temperatures during charge. Figure 7 shows that, for slightly insulated cells, temperature reaches 25 K above the ambient temperature (fluid at 20°C) at the end of the CC phase. On the positive side, the anode potential remains above 42 mV thanks to improved dynamics at higher temperature.

Immersion cooling, as shown in Figure 8, improves thermal management, i.e., the ability to bring the temperature of cells to a desired reference. There is no decrease in charging time compared with passive cooling when charging at 1C because temperature or electrochemical limits are not achieved in both passive or immersion. Special care should be taken not to cross the anode potential limits at lower temperatures and higher currents. This is illustrated in Figure 8, showing an anode potential margin of 18 mV. Depending on the expected fidelity of the electrochemical model, this may not be sufficient to ensure total lithium plating avoidance. In this case 4 K of peak cell temperature above ambient is achieved. Although a higher fluid flowrate is possible, the temperature reduction due to improved heat transfer will lead to a further drop in anode potential, and therefore higher risk of plating.

DOI 10.3384/ecp204121

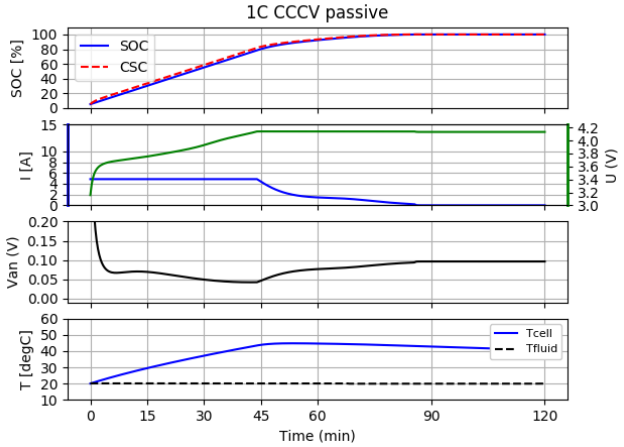

Figure 7. 1C-CCCV, single cell, passive cooling (T_{fluid} refers here to the environmental temperature)

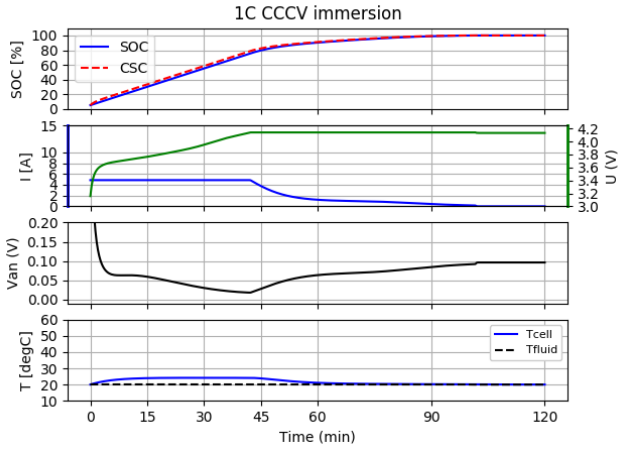

Figure 8. 1C-CCCV, single cell, immersion cooling

4.1.2 C-rate comparison

An increase in C-rate improves charging time significantly, from 45 min at 1C to 26 min at 2C (from 7.5% to 80% SOC). Only 5 mV of margin w.r.t. plating, and 33°C peak temperature set a limit in performance for safety and lifetime, but again model inaccuracies and cell-to-cell variations at BOL would encourage additional improvements to this profile, specially when considering charge at pack level.

4.1.3 Optimal constrained profile, 2C maximum C-rate

When constraints are present (40 mV for the anode potential, 45°C), the only way to reduce the charging time is to increase the fluid temperature so that the cell properties are enhanced. Figure 10 shows the calculated optimal current and temperature profile, which brings the charging time to 28 min, only 8% higher than the 2C-CCCV profile. The fluid temperature can vary +25/-10 K around the nominal value 20°C. It is worth noting the optimal trajectory of the

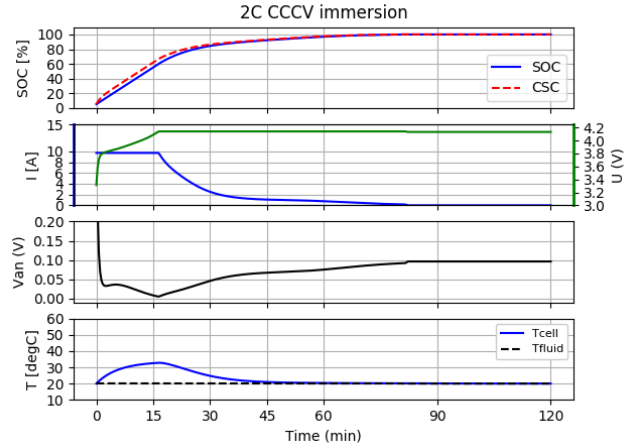

Figure 9. 2C-CCCV, single cell, immersion cooling

fluid temperature, which brings the temperature of the cell to the maximum level after a series of swings, and finally brings the cell to the nominal value even before the charge is completed. This of course depends on the controller setup, i.e., the weightings of the cost function. It must be noted that the time derivatives of the fluid temperature are limited in practice, for example, by the heating/cooling devices mounted on the vehicle. The consideration of such limits are beyond the scope of this work. If the fluid temperature is kept at 20°C at all times, the charging time increases to 44 min, just above the 1C-CCCV protocol.

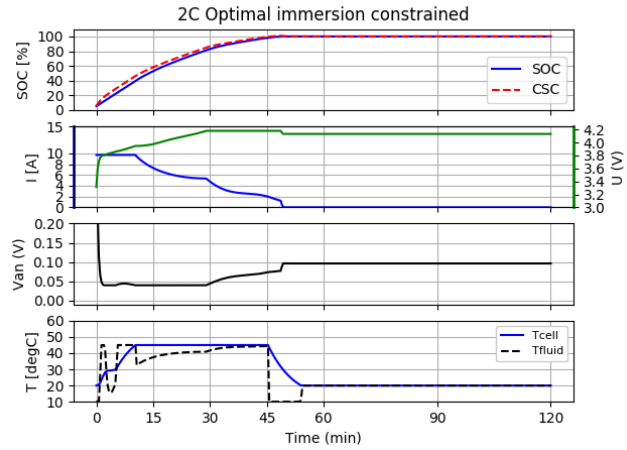

Figure 10. 2C Optimal profile, immersion cooling with temperature control

4.2 Pack level offline charge optimization

The obtained profiles are valid only for a pack where all the cells face the same boundary conditions, which in practice is generally not possible. The optimization algorithm can control the temperatures of all the cells (provided the first and last cell hold the extreme temperature values), as well as the temperature spread in the pack. For simplicity, we control the first and last cell's temperature,

as well as the absolute value of their temperature difference (T_{spread}).

4.2.1 No inlet fluid temperature control, no temperature spread control

We present first the case in which a pack is charged and only the current is manipulated. The only constraint that is not considered is the temperature spread. The maximum temperature is nevertheless not active, while the anode potential constraint is active for most of the charge, before the CV phase begins at about 53 min. The charging time (7.5%-80% SOC) is 44 min.

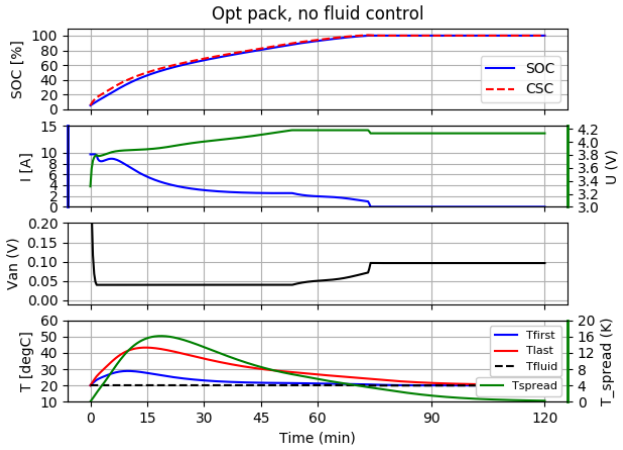

Figure 11. 2C Optimal profile, immersion cooling at pack level without fluid temperature control

4.2.2 Fluid temperature control, temperature spread control option

When the fluid temperature is amenable to manipulation, results become more interesting. Charging time is reduced to 34 min (Figure 12) when temperature spread is not included, and 36 min otherwise (Figure 13), which indicates that controlling temperature spread is marginally difficult if the inlet temperature can be controlled. These values are 21% and 29% higher than the single cell case. Incidentally, the maximum cell temperature constraint becomes active at some point due to increased inlet fluid temperature. Further limitation of the pack temperature spread down to 5 K leads to a charging time of 43 min, a 20% increase.

4.3 Pack level NMPC scheme

The results concerning the online fast charge optimization using NMPC are presented in this section. Some implementation details to be taking into account when utilizing this scheme on a real battery pack are also discussed. Figure 14 represents the same offline problem described in the last example (pack level constrained optimization with manipulated fluid temperature), now from a more realistic perspective. It should be noted, notwithstanding, that further limitations in pressure drop and fluid temperature

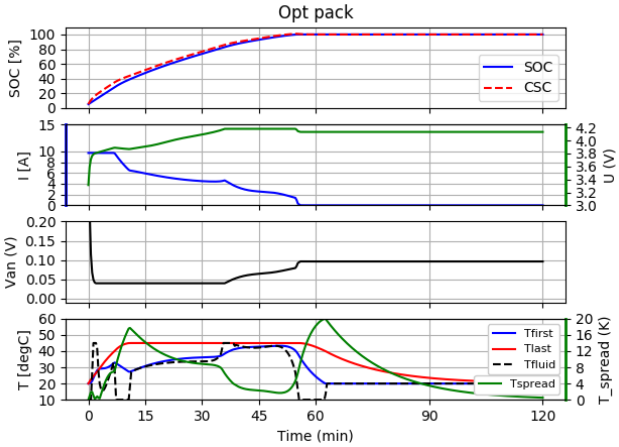

Figure 12. 2C Optimal profile, immersion cooling at pack level with fluid temperature

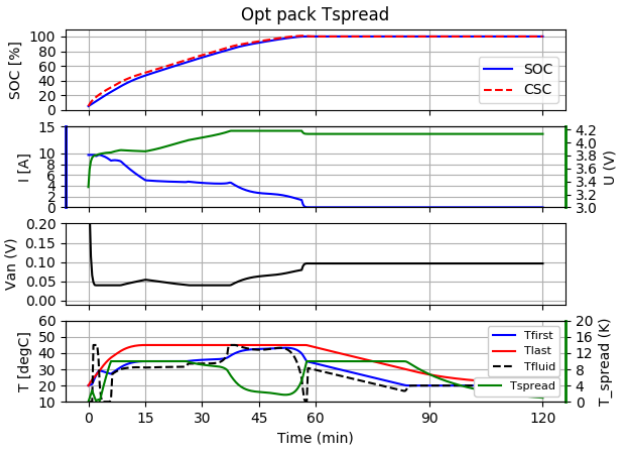

Figure 13. 2C Optimal profile, immersion cooling at pack level with fluid temperature and temperature spread control

ramps may slow down the overall charging operation.

The control horizon chosen in this work is 1000s, i.e., 100 steps of 10s each. The total computational time per step remained over the complete integration loop below 2 s for the device used (Windows system, processor Intel i7, 32 GB RAM, overall usage less than 20%). The total charging time (7.5%-80% SOC) is slightly increased up to 37 min. If the control horizon decreases to 100s, the computational time is reduced ten-fold, but the myopia of the controller leads to a charging time of 63 min, not being able to avoid temperature constraint saturation. This highlights the need for sufficient computing power.

Another limitation arises from model inaccuracies in the cool-down part after the charge (beyond 60 min), which leads to an increased temperature spread that would violate the controller's constraints. This helps us introducing how the scheme leads to constraint saturation when feeding back the plant's actual temperatures. Without explicit handling of such saturation, state values of the plant

DOI 10.3384/ecp204121

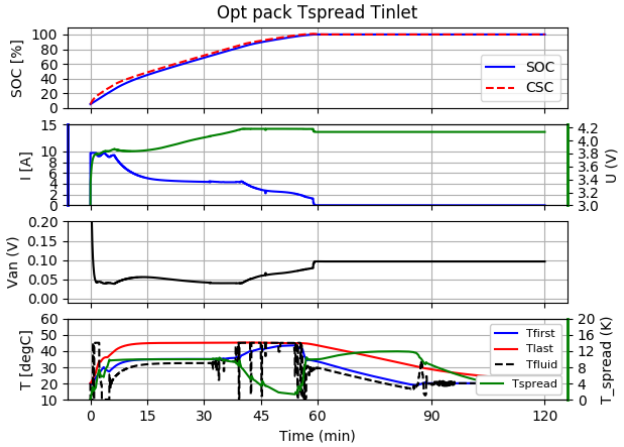

Figure 14. 2C NMPC profile, immersion cooling at pack level with temperature spread and temperature spread control

may initialize the optimization problem from an infeasible point. Correcting the state slightly to always stay within the limits of the saturation is proposed for the maximum temperature, which leads in this problem to satisfactory results, as seen in Figure 14, since plant and prediction models similar dynamics. However, it is clear from this figure that the temperature spread is violated during the cool-down phase. Saturation is resolved by fixing either the minimum or maximum temperature, and afterwards the remaining one considering the limited spread. Not dealing with spread saturation leads to slightly higher charging time (38 min), and future work will be devoted to examine better options to include a robust approach that ensures feasibility.

5 Conclusions

Fast charging of battery packs present a rich set of design and operational challenges. In this paper, it has been shown that active thermal management is critical to achieve competitive charging speeds in combination with optimization-based control algorithms. Unlike previous works tackling only single cell level operation, this work has demonstrated that the objective of less than 20 min pack-level fast charge (0-80%) is not yet attainable. In fact, we proved that even with high-effective immersion cooling and optimization-based algorithms, the charging time from cell to pack is expected to increase by more than 40%. In summary, further improvements from the current state-of-the-art on cell design, cell-to-pack integration, and thermal management are needed. Ongoing extensions for the current formulation include the addition of a flow-pressure model and a more realistic approach of the available heating/cooling power for thermal management, so that constraints in pack pressure drop, volumetric flowrate, and fluid inlet temperature ramps can be applied.

References

Andersson, Joel et al. (2011). "Integration of CasADi and JModelica. org". In: *Proceedings of the 8th International Modelica Conference; March 20th-22nd; Technical Univeristy; Dresden; Germany*. 063. Linköping University Electronic Press, pp. 218–231.

Barreras, Jorge Varela, Trishna Raj, and David A Howey (2018). "Derating strategies for lithium-ion batteries in electric vehicles". In: *IECON 2018-44th Annual Conference of the IEEE Industrial Electronics Society*. IEEE, pp. 4956–4961.

Batteh, John and Michael Tiller (2009). "Implementation of an extended vehicle model architecture in modelica for hybrid vehicle modeling: development and applications". In: *Proceedings of the 7th International Modelica Conference; Como; Italy; 20-22 September 2009*. 043. Linköping University Electronic Press, pp. 823–832.

Blochwitz, Torsten et al. (2011). "The functional mockup interface for tool independent exchange of simulation models". In: *Proceedings of the 8th international Modelica conference*. Linköping University Press, pp. 105–114.

Bouvy, Claude et al. (2012). "Holistic vehicle simulation using Modelica-An application on thermal management and operation strategy for electrified vehicles". In: *Proceedings of the 9th International Modelica Conference; September 3-5; 2012; Munich; Germany*. 076. Linköping University Electronic Press, pp. 264–270.

Brembeck, Jonathan and Sebastian Wielgos (2011). "A real time capable battery model for electric mobility applications using optimal estimation methods". In: *Proceedings of the 8th International Modelica Conference; March 20th-22nd; Technical Univeristy; Dresden; Germany*. 063. Linköping University Electronic Press, pp. 398–405.

Camacho, Eduardo F and Carlos Bordons Alba (2013). *Model predictive control*. Springer science & business media.

Chaturvedi, Nalin A et al. (2010). "Algorithms for advanced battery-management systems". In: *IEEE Control systems magazine* 30.3, pp. 49–68.

Chen, Chang-Hui et al. (2020). "Development of experimental techniques for parameterization of multi-scale lithium-ion battery models". In: *Journal of The Electrochemical Society* 167.8, p. 080534.

Couto, Luis D et al. (2016). "SOC and SOH estimation for Li-ion batteries based on an equivalent hydraulic model. Part I: SOC and surface concentration estimation". In: *2016 American control conference (ACC)*. IEEE, pp. 4022–4028.

Dao, Thanh-Son and Chad Schmitke (2015). "Developing Mathematical Models of Batteries in Modelica for Energy Storage Applications". In: *Proceedings of the 11th International Modelica Conference, Versailles, France, September 21-23, 2015*. 118. Linköping University Electronic Press, pp. 469–477.

Einhorn, M et al. (2011). "A modelica library for simulation of electric energy storages". In: *Proceedings of the 8th International Modelica Conference; March 20th-22nd; Technical Univeristy; Dresden; Germany*. 63. Linköping University Electronic Press, pp. 436–445.

Forman, Joel C et al. (2011). "Reduction of an electrochemistry-based li-ion battery model via quasi-linearization and pade approximation". In: *Journal of the Electrochemical Society* 158.2, A93.

Frank, Alexander et al. (2022). "Impact of Current Collector Design and Cooling Topology on Fast Charging of Cylindrical Lithium-Ion Batteries". In: *ECS Advances* 1.4, p. 040502.

Gerl, Johannes et al. (2014). "A Modelica Based Lithium Ion Battery Model". In: *Proceedings of the 10 th International Modelica Conference; March 10-12; 2014; Lund; Sweden*. 096. Linköping University Electronic Press, pp. 335–341.

Groß, Christian and Andrey Golubkov (2021). "A Modelica library for Thermal-Runaway Propagation in Lithium-Ion Batteries". In: *14th Modelica Conference 2021*.

Janczyk, Leonard et al. (2016). "Validation of a Battery Management System based on AUTOSAR via FMI on a HiL platform". In: *The First Japanese Modelica Conferences, May 23-24, Tokyo, Japan*. 124. Linköping University Electronic Press, pp. 87–94.

Kasper, Manuel et al. (2023). "Calibrated Electrochemical Impedance Spectroscopy and Time-Domain Measurements of a 7 kWh Automotive Lithium-Ion Battery Module with 396 Cylindrical Cells". In: *Batteries & Supercaps* 6.2, e202200415.

Kastler, Helmut and Kilian Menzl (2021). "Effective Battery Design and Integration of Cylindrical Cells for High Power Applications". In: *CTI SYMPOSIUM 2019: 18th International Congress and Expo 9-12 December 2019, Berlin, Germany*. Springer, pp. 283–293.

Keyser, Matthew et al. (2017). "Enabling fast charging–Battery thermal considerations". In: *Journal of Power Sources* 367, pp. 228–236.

Kreisel Electric (2023). *We drive the future*. http : / / www . kreiselelectric.com. Accessed: 2023-06-14.

Krüger, Imke, Martin Sievers, and Gerhard Schmitz (2009). "Thermal modeling of automotive lithium ion cells using the finite elements method in modelica". In: *Proceedings of the 7th International Modelica Conference; Como; Italy; 20-22 September 2009*. 043. Linköping University Electronic Press, pp. 1–8.

Li, Yang et al. (2019). "Development of a degradation-conscious physics-based lithium-ion battery model for use in power system planning studies". In: *Applied Energy* 248, pp. 512–525. ISSN: 0306-2619. DOI: https://doi.org/10.1016/j.apenergy.2019.04.143. URL: https://www.sciencedirect.com/science/article/pii/S0306261919308049.

Magnusson, Fredrik and Johan Åkesson (2015). "Dynamic optimization in JModelica. org". In: *Processes* 3.2, pp. 471–496.

Manwell, James F. and Jon G. McGowan (1993). "Lead acid battery storage model for hybrid energy systems". In: *Solar Energy* 50.5, pp. 399–405. ISSN: 0038-092X. DOI: https://doi.org/10.1016/0038-092X(93)90060-2. URL: https://www.sciencedirect.com/science/article/pii/0038092X93900602.

Pesaran, Ahmad A (2002). "Battery thermal models for hybrid vehicle simulations". In: *Journal of power sources* 110.2, pp. 377–382.

Romero, Alberto, Alejandro Goldar, Luis D Couto, et al. (2019). "Fast charge of Li-ion batteries using a two-layer distributed MPC with electro-chemical and thermal constraints". In: *2019 18th European Control Conference (ECC)*. IEEE, pp. 1796–1803.

Romero, Alberto, Alejandro Goldar, and Emanuele Garone (2019). "A model predictive control application for a constrained fast charge of lithium-ion batteries". In: *Proceedings of the 13th International Modelica Conference, Regensburg, Germany, March 4–6, 2019*. 157. Linköping University Electronic Press.

Sievers, Martin, Uwe Sievers, and Samuel S Mao (2010). "Thermal modelling of new Li-ion cell design modifications". In: *Forschung im Ingenieurwesen* 74.4, pp. 215–231.

Spike, Jonathan et al. (2015). "Holistic Virtual Testing and Analysis of a Concept Hybrid Electric Vehicle Model". In: *Proceedings of the 11th International Modelica Conference, Versailles, France, September 21-23, 2015*. 118. Linköping University Electronic Press, pp. 537–545.

Stüber, Moritz (2017). "Simulating a variable-structure model of an electric vehicle for battery life estimation using modelica/dymola and python". In: *Proceedings of the 12th International Modelica Conference, Prague, Czech Republic, May 15-17, 2017*. 132. Linköping University Electronic Press, pp. 291–298.

Tomaszewska, Anna et al. (2019). "Lithium-ion battery fast charging: a review". In: *ETransportation* 1, p. 100011.

Uddin, Kotub and Alessandro Picarelli (2014). "Phenomenological Li ion battery modelling in Dymola". In: *Proceedings of the 10 th International Modelica Conference; March 10-12; 2014; Lund; Sweden*. 96. Linköping University Electronic Press, pp. 327–334.

Wang, Jianguo et al. (2020). "Effect analysis on thermal behavior enhancement of lithium–ion battery pack with different cooling structures". In: *Journal of energy storage* 32, p. 101800.

Wassiliadis, Nikolaos et al. (2022). "Quantifying the state of the art of electric powertrains in battery electric vehicles: Range, efficiency, and lifetime from component to system level of the Volkswagen ID. 3". In: *ETransportation* 12, p. 100167.

Yang, Xiao-Guang, Teng Liu, et al. (2019). "Asymmetric temperature modulation for extreme fast charging of lithium-ion batteries". In: *Joule* 3.12, pp. 3002–3019.

Yang, Xiao-Guang and Chao-Yang Wang (2018). "Understanding the trilemma of fast charging, energy density and cycle life of lithium-ion batteries". In: *Journal of Power Sources* 402, pp. 489–498.

Yin, Yilin and Song-Yul Choe (2020). "Actively temperature controlled health-aware fast charging method for lithium-ion battery using nonlinear model predictive control". In: *Applied energy* 271, p. 115232.